

Surface-enhanced Raman spectroscopy with monolithic nanoporous gold disk substrates

Ji Qi, Pratik Motwani, Mufaddal Gheewala, Christopher Brennan, John C. Wolfe,

and Wei-Chuan Shih

Fabrication processes of nanoporous gold disks (NPGDs)

The NPGD fabrication process is shown in Fig. S1. First, a 300 nm thick gold layer is sputter-deposited on a silicon wafer followed by a 75 nm Au/Ag alloy film using DC-magnetron with a 25 mm source (Lesker). The gold film was deposited using a 99.99 % pure gold target (Royal Canadian Mint). The Au/Ag alloy film was deposited using an alloy target with Au:Ag ratio of 28:72 (ACI Alloys). The Ar sputtering pressure and power were 5 mTorr and 50 W, respectively. A magnetic virtual anode, adapted from the cylindrical magnetron, was used to prevent electron bombardment of the growing film. The deposition rates for the gold and the alloy films were 37.5 nm/min and 25 nm/min, respectively.

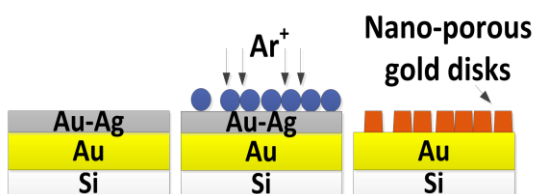


Fig. S1. Fabrication process flow: (a) Au/Ag and Au film stack on silicon substrate; (b) Au/Ag by Ar⁺ sputter etching using drop-coated polystyrene beads as a mask; (c) removal of polystyrene beads and free corrosion in nitric acid to form nanoporous gold discs.

Next, 500 nm polystyrene (PS) beads (Polysciences, Inc.) are drop-coated onto the alloy film, followed by RF-sputter etching using the PS beads as an etch mask. Sputter-etching was carried out in a homemade reactor with a 150 mm cathode using 99.999% pure argon gas. The power density and argon gas pressure were 0.057 W/cm^2 and 2 mTorr, respectively. The etch rate of the alloy film was calibrated by scanning electron microscopy to be $\sim 30 \text{ nm/min}$. The etching step produces completely isolated alloy disks sitting on $\sim 65 \text{ nm}$ thick solid gold bases with a remaining underlying gold film $\sim 235 \text{ nm}$ thick (Fig. 2(a)). The PS spheres are then removed by solvent and sonication. Finally, NPG is formed selective dissolution of the silver using a 1 sec dip in 70% nitric acid followed by deionized water rinse and nitrogen dry.

Figure S2(a) shows the scanning electron micrograph (SEM) of the PS bead residues covering an etched alloy and gold film stack to confirm the thickness and the effectiveness of PS beads as the etch mask. The boundary between the alloy and gold base is visible in the high magnification image of Fig. S2(b). The top surface of NPGD is revealed after the removal of the PS beads and nitric acid corrosion as shown in Fig. S2(c). Here we can observe the ultra-fine nanoporous network similar to that obtained from unpatterned NPG thin films (Fig. S2(d)) fabricated by the same selective dissolution procedure. Cracks are seen in both the NPGD and unpatterned NPG films due to surface stress.

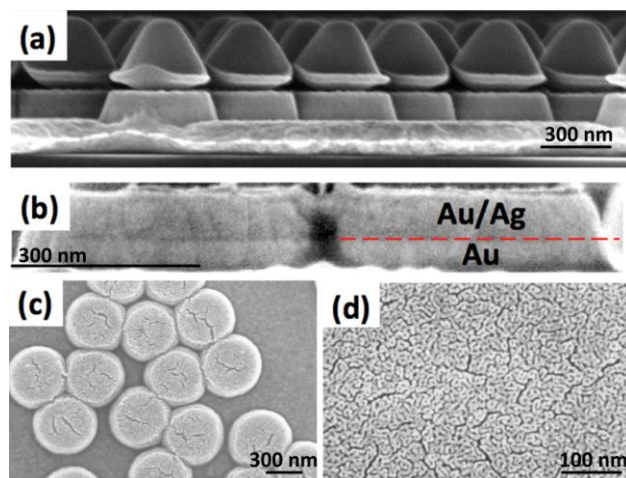


Fig. S2. NPGD fabrication: (a) etched Au/Ag alloy disks on Au bases; (b) sideview of alloy disks to show visible boundary between Au/Ag alloy and the Au base; (c) NPGD topview; (d) unpatterned NPG thin film.

Large-area SERS mapping with corresponding SEM and optical micrographs

We have performed large-area SERS mapping on several regions on the NPGD samples and obtained similar results as shown in the manuscript (cf., Fig. 3-6). The additional map results are shown in Fig. S3.

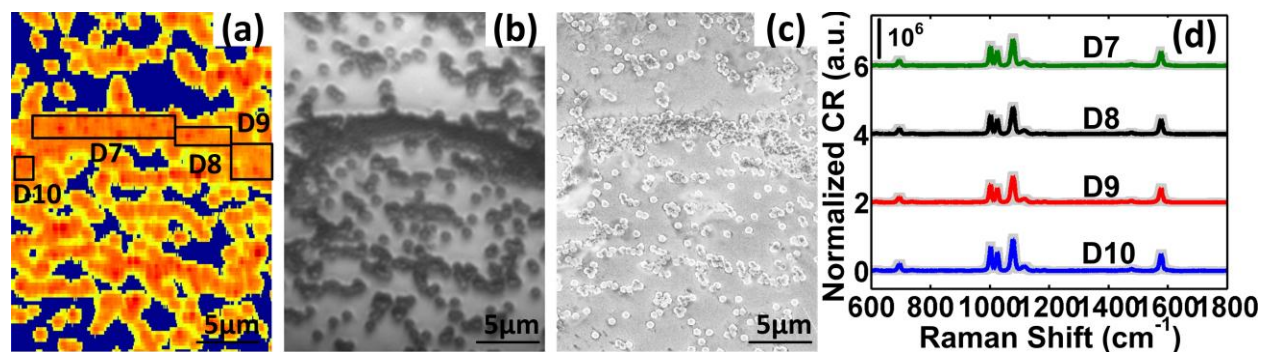


Fig. S3. (a) SERS map of NPGD by the line-scan Raman system; (b) visual image and (c) SEM image; (d) average spectra with ± 1 standard deviation in gray shadows from 4 different locations shown in (a).

To demonstrate NPGD's potential in fast detection of trace molecular amounts, we have performed a series of experiments by varying the CCD integration time. In Fig. S4(a), we show the results with integration time from 1 sec to 25 msec. The SNR (dB) vs. integration time is plotted in the inset of Fig S4(a), suggesting that a single NPGD coated with BT SAM can be detected with an SNR ~ 13 dB in 25 msec (the shortest integration time allowable in our system). The laser power density was $170 \mu\text{W}/\mu\text{m}^2$.

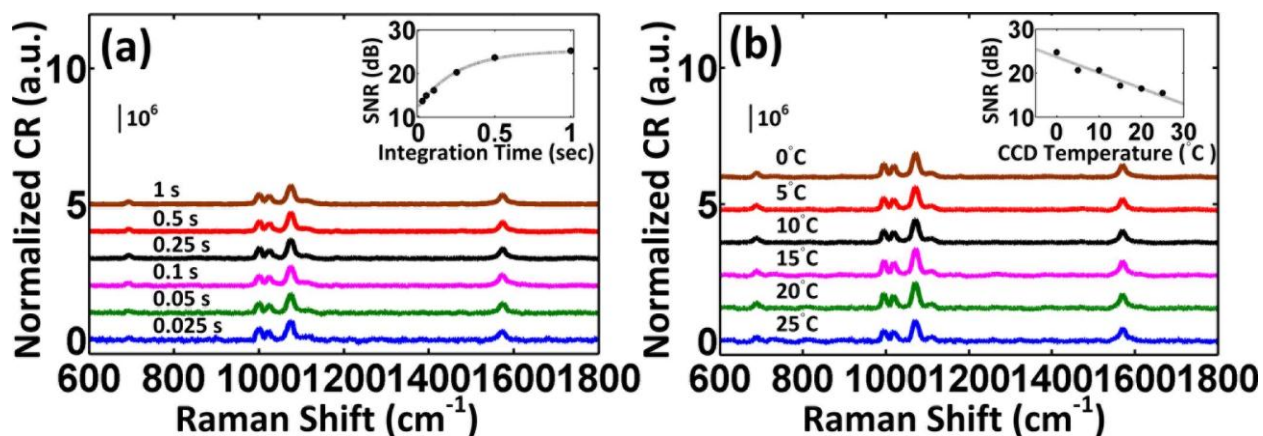


Fig. S4. Normalized count rate (CR) and SNR from a single NPGD vs. CCD integration times (a) and CCD temperatures (b).

All the previous results were obtained using a CCD cooled down to -70 °C. Next, we explore the detection capability of a single NPGD with various CCD temperatures with results shown in Fig. S4(b). The SNR vs. CCD temperature is plotted in the inset of Fig. S4(b), suggesting NPGD can be detected with SNR ~ 14 dB at CCD temperature as high as 25 °C. The laser power density was $1.7 \text{ mW}/\mu\text{m}^2$ and the integration time was 1 sec.